

## Asymmetric Distribution of Cholesterol in Unilamellar Vesicles of Monounsaturated Phospholipids

Norbert Kučerka,<sup>\*,†,‡</sup> Mu-Ping Nieh,<sup>†</sup> and John Katsaras<sup>\*,†,§,⊥</sup>

<sup>†</sup>Canadian Neutron Beam Centre, National Research Council, Chalk River, Ontario K0J 1J0, Canada, <sup>‡</sup>Department of Physical Chemistry of Drugs, Faculty of Pharmacy, Comenius University, 832 32 Bratislava, Slovakia, <sup>§</sup>Department of Physics, Brock University, St. Catharines, Ontario L2S 3A1, Canada, and <sup>⊥</sup>Guelph-Waterloo Physics Institute and Biophysics Interdepartmental Group, University of Guelph, Guelph, Ontario N1G 2W1, Canada

Received June 5, 2009. Revised Manuscript Received July 22, 2009

We have studied the effect of cholesterol on curved bilayers using 600 Å unilamellar vesicles made of monounsaturated lipids. From small-angle X-ray scattering experiments we were able to detect an asymmetric distribution of lipid densities across certain bilayers. We discovered that, with the exception of diC24:1PC bilayers, monounsaturated diacylphosphatidylcholine lipids (diC<sub>n</sub>:1PC, *n* = 14, 16, 18, 20, and 22) form symmetric bilayers. However, the addition of 44 mol % cholesterol resulted in some of these bilayers (i.e., *n* = 14, 16, and 18) to become asymmetric, where cholesterol was found to distribute unequally between the bilayer's two leaflets. This finding is potentially of relevance to biological membranes made up of different types of lipids and whose local curvature may be dictated by lipid composition.

## Introduction

Membrane curvature is an essential feature for inter- and intracellular communication as various cell membrane functions (i.e., budding and fusion) are performed when specific geometric conditions are present.<sup>1,2</sup> Changes to a cell's membrane local curvature have been observed to drive the lateral organization in model systems<sup>3</sup> and may also lead to lateral heterogeneities in cell membranes.<sup>4</sup> A membrane's local curvature and its lateral organization are often modulated by membrane-associated proteins; on the other hand, curvature alone enables mechanisms for organizing mobile membrane molecules.<sup>2</sup> Of note is that membrane lateral heterogeneities in model systems have been observed to produce local variations in membrane curvature.<sup>5,6</sup>

There have been numerous studies on single-component model membranes assessing the influence of curvature on a membrane's thermodynamic properties and its asymmetry.<sup>7–13</sup> Meanwhile, similar studies of multicomponent membranes have addressed

questions related to lipid miscibility.<sup>14–16</sup> Data from these studies show that an increase in membrane curvature results in a shift and broadening of the phase transition temperature of single-component vesicles and influences the miscibility and bilayer asymmetry in mixed lipid systems.

Though it is not known how a cell regulates the lateral organization of its plasma membrane, cholesterol-dependent phase separation is believed to play a key role.<sup>2</sup> The connection between cholesterol content and membrane thickness has been suggested in the sorting and trafficking of membrane proteins along the exocytic pathway through the Golgi apparatus. For example, transmembrane domains of plasma membrane proteins are, on average, five amino acids longer than those of the Golgi, and membranes along the exocytic pathway increasingly thicken from the endoplasmic reticulum to the plasma membrane.<sup>17</sup> This progressive membrane thickening has been correlated with a concomitant increase in cholesterol content along the secretory pathway, suggesting that cholesterol determines the membrane's thickness and controls the destination of proteins based on hydrophobic matching.

We have recently confirmed that cholesterol increases the thickness of bilayers prepared from monounsaturated phospholipids with 14–22 carbon hydrocarbon chains.<sup>18</sup> In addition, it has been shown that the distribution of cholesterol across bilayers is not necessarily symmetric, especially in disordered bilayers.<sup>19</sup> The modulation of local lipid composition in asymmetric membranes has been discussed as a mechanism by which cells can actively regulate protein function.<sup>20</sup> It has also been shown that the bilayer's leaflets are strongly coupled, even in the presence of

\*Corresponding authors. E-mail: Norbert.Kucerka@nrc.gc.ca; John.Katsaras@nrc.gc.ca.

- (1) McMahon, H. T.; Gallop, J. L. *Nature* **2005**, *438*, 590–596.
- (2) Parthasarathy; Raghuvveer; Groves; Jay, T. *Soft Matter* **2007**, *3*, 24–33.
- (3) Roux, A.; Cuvelier, D.; Nassoy, P.; Prost, J.; Bassereau, P.; Goud, B. *EMBO J.* **2005**, *24*, 1537–1545.
- (4) van Meer, G.; Vaz, W. L. *EMBO Rep.* **2005**, *6*, 418–419.
- (5) Baumgart, T.; Hess, S. T.; Webb, W. W. *Nature* **2003**, *425*, 821–824.
- (6) Bacia, K.; Schwill, P.; Kurzchalia, T. *Proc. Natl. Acad. Sci. U.S.A.* **2005**, *102*, 3272–3277.
- (7) Marsh, D.; Watts, A.; Knowles, P. F. *Biochim. Biophys. Acta* **1977**, *465*, 500–514.
- (8) van Dijk, P. W.; de Kruijff, B.; Aarts, P. A.; Verkleij, A. J.; de Gier, J. *Biochim. Biophys. Acta* **1978**, *506*, 183–191.
- (9) Gruenewald, B.; Stankowski, S.; Blume, A. *FEBS Lett.* **1979**, *102*, 227–229.
- (10) Eigenberg, K. E.; Chan, S. I. *Biochim. Biophys. Acta* **1980**, *599*, 330–335.
- (11) Boni, L. T.; Minchey, S. R.; Perkins, W. R.; Ahl, P. L.; Slater, J. L.; Tate, M. W.; Gruner, S. M.; Janoff, A. S. *Biochim. Biophys. Acta* **1993**, *1146*, 247–257.
- (12) Nagano, H.; Nakanishi, T.; Yao, H.; Ema, K. *Phys. Rev. E* **1995**, *52*, 4244–4250.
- (13) Kučerka, N.; Pencser, J.; Sachs, J. N.; Nagle, J. F.; Katsaras, J. *Langmuir* **2007**, *23*, 1292–1299.
- (14) Nordlund, J. R.; Schmidt, C. F.; Dicken, S. N.; Thompson, T. E. *Biochemistry* **1981**, *20*, 3237–3241.

- (15) Brumm, T.; Jorgensen, K.; Mouritsen, O. G.; Bayerl, T. M. *Biophys. J.* **1996**, *70*, 1373–1379.
- (16) Pencser, J.; Jackson, A.; Kučerka, N.; Nieh, M. P.; Katsaras, J. *Eur. Biophys. J.* **2008**, *37*, 665–671.
- (17) Bretscher, M. S.; Munro, S. *Science* **1993**, *261*, 1280–1281.
- (18) Gallová, J.; Uhríková, D.; Kučerka, N.; Teixeira, J.; Balgavý, P. *Biochim. Biophys. Acta* **2008**, *1778*, 2627–2632.
- (19) Kučerka, N.; Perlmutter, J. D.; Pan, J.; Tristram-Nagle, S.; Katsaras, J.; Sachs, J. N. *Biophys. J.* **2008**, *95*, 2792–2805.
- (20) Collins, M. D.; Keller, S. L. *Proc. Natl. Acad. Sci. U.S.A.* **2008**, *105*, 124–128.

phase separation, and the effects of membrane curvature and protein coupling have been discussed. Furthermore, Parthasarathy et al.<sup>21</sup> suggested the coupling between local curvature and membrane chemical composition as a means of controlling the spatial organization of membrane components. Another important consideration is the nature of the intracellular and extracellular media, which can result in localized structural changes through differences in hydration.

Here we show that cholesterol can induce membrane asymmetry. On the basis of characteristic features observed in small-angle X-ray scattering (SAXS) data, we have identified the asymmetric distribution of cholesterol in bilayers made of diC14:1PC, diC16:1PC, and diC18:1PC lipids, but not in bilayers of diC20:1PC, diC22:1PC, and diC24:1PC. This agrees well with MD simulations which indicated that cholesterol moves much more freely between a bilayer's leaflets, when bilayers are disordered (e.g., short monounsaturated lipids).<sup>19</sup> We speculate that even a small effect in bilayer curvature can result in the anisotropic distribution of cholesterol in disordered bilayers.

## Materials and Methods

**Sample Preparation.** Synthetic 1,2-dimyristoleoyl-*sn*-glycero-3-phosphatidylcholine (diC14:1PC), 1,2-dipalmitoleoyl-*sn*-glycero-3-phosphatidylcholine (diC16:1PC), 1,2-dioleoyl-*sn*-glycero-3-phosphatidylcholine (diC18:1PC), 1,2-dieicosenoyl-*sn*-glycero-3-phosphatidylcholine (diC20:1PC), 1,2-dierucoyl-*sn*-glycero-3-phosphatidylcholine (diC22:1PC), and 1,2-dinervonoyl-*sn*-glycero-3-phosphatidylcholine (diC24:1PC) were purchased from Avanti Polar Lipids (Alabaster, AL) and used without further purification. Cholesterol was obtained from Sigma-Aldrich (St. Louis, MO). All other chemicals were of reagent grade.

Lipids were cosolubilized in chloroform with 44 mol % (molar ratio of 0.8) cholesterol in glass vials. Chloroform was then evaporated under a stream of nitrogen gas followed by exposure to vacuum. The resultant lipid film was then dispersed in 18 M $\Omega$ ·cm water (Millipore) to a total lipid concentration  $\sim$ 20 mg/mL. 600 Å diameter unilamellar vesicles (ULVs) were prepared according to ref 13. Dynamic light scattering measurements performed on similar systems suggested relative polydispersities (Gaussian width/ULV radius) of  $\sim$ 25%.<sup>13</sup> When analyzing the data, compositional variation among ULVs was not taken into account. Prior experience has shown that compositionally equivalent ULVs are formed when they are extruded at a temperature at which all of the ULV's components are in the fluid phase.<sup>16</sup>

**Small-Angle X-ray Scattering.** Small-angle X-ray scattering (SAXS) measurements were performed at Cornell's High Energy Synchrotron Source (CHESS) G-1 station. A 1.234 Å wavelength ( $\lambda$ ) X-ray beam of size  $0.3 \times 0.3$  mm<sup>2</sup> was used. Scattered X-rays were detected using a 1024  $\times$  1024 pixel array FLICAM charge-coupled device (CCD), with 69.78  $\mu$ m linear dimension pixels. The sample-to-detector distance (SDD) was 418.6 mm (determined by using silver behenate standard), resulting in a total scattering vector [ $q = 4\pi/\lambda \sin(\theta/2)$ , where  $\lambda$  is the wavelength and  $\theta$  is the scattering angle] of  $0.06 < q < 0.65$  Å<sup>-1</sup>. Samples were taken up in 1.5 mm quartz capillaries, which were placed in a temperature-controlled multipositional sample holder for experiment. 2D images of scattered intensities were "dezingered" using two consecutive 10 s exposures and corrected using calibration files supplied to us by CHESS. Each data set was normalized using the incident beam intensity, which was measured using a standard ion chamber. The background resulting from water and air scattering was subtracted according to the procedure described in ref 13.

**Structural Model of a Lipid Bilayer.** X-ray scattering is mostly sensitive to the electron dense phosphate moieties found in

a lipid molecule's headgroup region. On the other hand, the least electron dense region is the center of the bilayer as a result of extensive thermal motion by the terminal methyl group. These two bilayer features are modeled using Gaussians with positive (i.e., phosphate) or negative amplitude (i.e., terminal methyls). More precisely, the headgroup is modeled with two positive amplitude Gaussians, while the terminal methyl trough is described by a single negative Gaussian (see Supporting Information for more details). The smooth transition between the hydrophilic and hydrophobic regions is achieved by using error functions similar to ones used in more advanced models.<sup>22</sup> Although it is possible to use more complex models, it is also important to minimize the number of free parameters, thus avoiding ambiguous results. Here we focus our attention on the presence or absence of bilayer asymmetry and not on the precise structure of the bilayer. Bilayer asymmetry in the model is accomplished by allowing the headgroup peaks in each bilayer leaflet to assume different positions and amplitudes. Since this nearly doubles the number of fitting parameters, it is desirable to keep the model reasonably simple. However, by doing so this precludes the possibility of a detailed bilayer structure.

**Effect of Bilayer Asymmetry.** The scattering form factor for a symmetric bilayer is taken from the well-known Fourier transform of the electron density profile (EDP). This expression is given as

$$|F(q)| = \left| 2 \int_0^{D/2} \Delta\rho(z) \cos(qz) dz \right| \quad (1)$$

where  $\Delta\rho(z)$  is the electron density difference between the bilayer and the solvent, while the integration extends from the bilayer center to a point ( $D/2$ ) beyond where  $\Delta\rho(z) = 0$ . The behavior of  $|F(q)|$  for a typical symmetric lipid bilayer is characterized by periodic oscillations that go to zero. However, a lack of zero intensity indicates bilayer asymmetry, as can be deduced from the following expression of the Fourier transform

$$|F(q)| = \left( \left[ \int_{-D/2}^{D/2} \Delta\rho(z) \cos(qz) dz \right]^2 + \left[ \int_{-D/2}^{D/2} \Delta\rho(z) \sin(qz) dz \right]^2 \right)^{1/2} \quad (2)$$

This calculation corresponds to the complete form of the Fourier transform with a complex exponential.

## Results

**Single-Component Bilayers.** Scattering from isotropic ULV samples results in rings of scattering. These 2D data can then be easily converted into 1D scattering intensities plotted as a function of scattering vector  $q$ . When using ULVs, the  $q$  range in a SAXS experiment is typically  $< 0.6$  Å<sup>-1</sup>. The data shown in Figure 1 are of sufficient quality that they can be used in an analysis capable of producing a bilayer's precise structural properties, as was recently shown.<sup>22,23</sup> However, the focus of the present study is on the determination of bilayer asymmetry, rather than the structural details of a bilayer. In this case, bilayer asymmetry is readily detectable because of the distinct scattering features associated with this effect. Unlike asymmetric bilayers, scattering from symmetric structures contains the typical zero

(22) Kučerka, N.; Nagle, J. F.; Sachs, J. N.; Feller, S. E.; Penczer, J.; Jackson, A.; Katsaras, J. *Biophys. J.* **2008**, *95*, 2356–2367.

(23) Kučerka, N.; Gallová, J.; Uhríková, D.; Balgavý, P.; Bulacu, M.; Marrink, S. J.; Katsaras, J. *Biophys. J.* **2009**.

(21) Parthasarathy, R.; Yu, C. H.; Groves, J. T. *Langmuir* **2006**, *22*, 5095–5099.

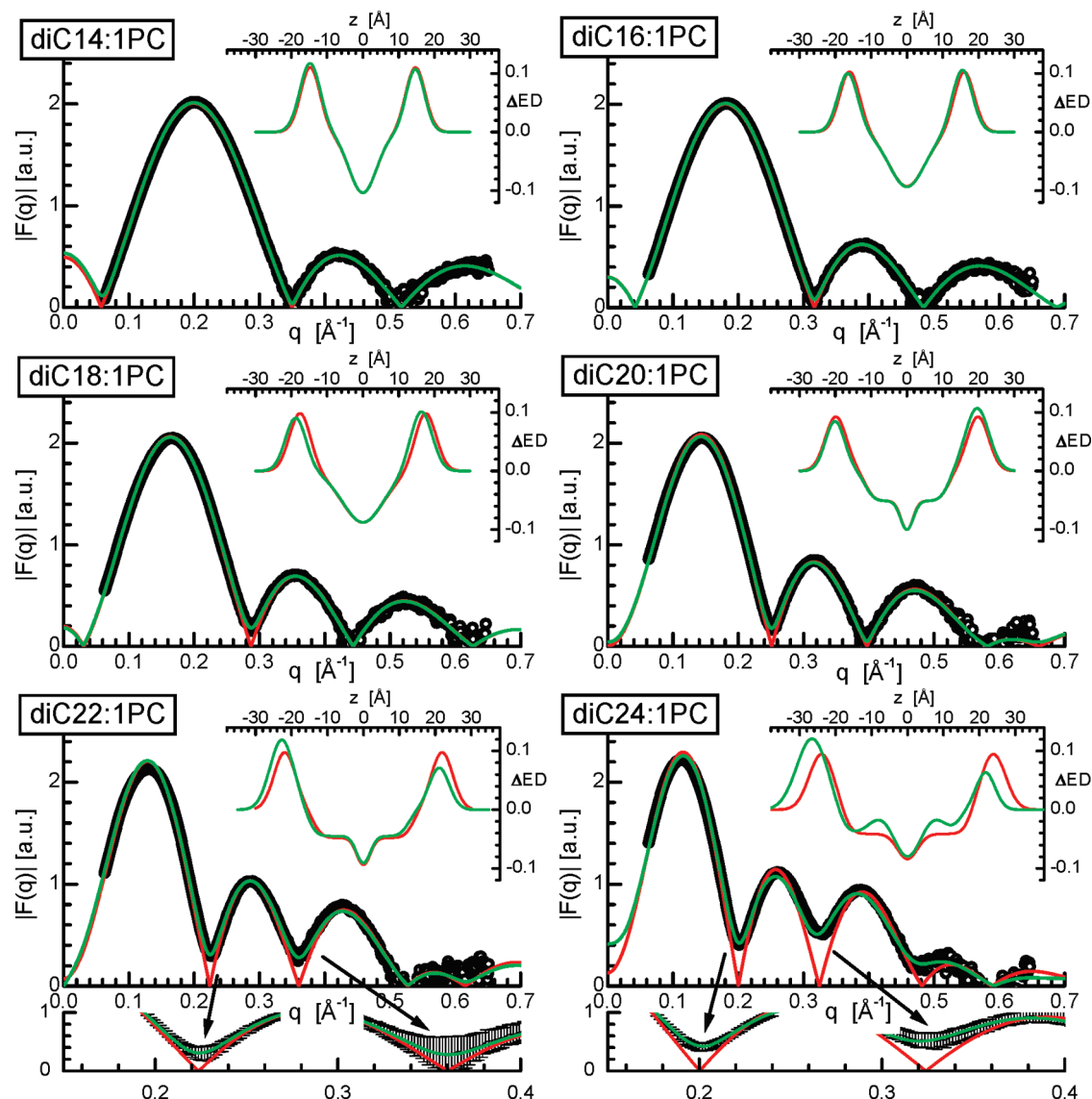


**Figure 1.** The solid lines are the best fit results to X-ray scattering form factors  $F(q)$  obtained for the various di-monounsaturated phosphatidylcholine bilayers at 30 °C. Inset graphs show the water-subtracted 1D electron density profiles. The red curves are best fits to the data using a symmetric bilayer model, while the green curves are best fits to the data using an asymmetric bilayer model. In the case of diC22:1PC and diC24:1PC bilayers, the data are expanded to include the associated error bars.

minima in the scattered intensity (Figure 1). Lipids with hydrocarbon chains up to 20 carbons readily form symmetric bilayers, and all four scattering curves associated with these lipids (Figure 1) exhibit distinct zero minima—this conclusion is also supported by 1D EDPs obtained by fitting the data in which the two bilayer leaflets were allowed to vary independently. As expected, for bilayers with hydrocarbon chains up to 20 carbons, the two models (i.e., symmetric and asymmetric) fit the data (within experimental error) equally well (Figure 1). Even in the case of the asymmetric model, the 1D EDPs are practically indistinguishable from the symmetric model results. In the case of the diC18:1PC bilayers, the fact that they are symmetric is known.<sup>13</sup>

The analysis of diC22:1PC bilayers proved to be somewhat problematic, even though there is a pronounced deviation of the minima from zero intensity. However, it should be pointed out that from the uncertainties in the data this deviation of the minima from zero is not statistically significant (Figure 1). Furthermore, the calculated EDPs, although somewhat different, reveal only marginal differences between symmetric and asymmetric

structures—based on the position of the headgroup peaks and their respective areas. The data presented here are also consistent with previously published data for the same bilayers,<sup>24</sup> where it was found that diC22:1PC bilayers are symmetric. We should state that in the case where asymmetric and symmetric bilayer models fit the data equally well (i.e., within experimental error) we will assume that the bilayers are symmetric.

The case for diC24:1PC bilayers, however, is very different. The scattering from diC24:1PC bilayers exhibit significant nonzero minima whose deviation are much greater than experimental error (see Figure 1). The calculated EDP for asymmetric bilayers shows a distinct shift in the phosphorylcholine peak position between the bilayer's two leaflets, as well as differences in their corresponding areas. The ratio between these two areas is  $\sim 3$ , and the difference in the peak positions is  $\sim 4$  Å. From these data it is clear that 600 Å diC24:1PCs ULVs form asymmetric bilayers.

(24) Kučerka, N.; Tristram-Nagle, S.; Nagle, J. F. *J. Membr. Biol.* **2005**, *208*, 193–202.

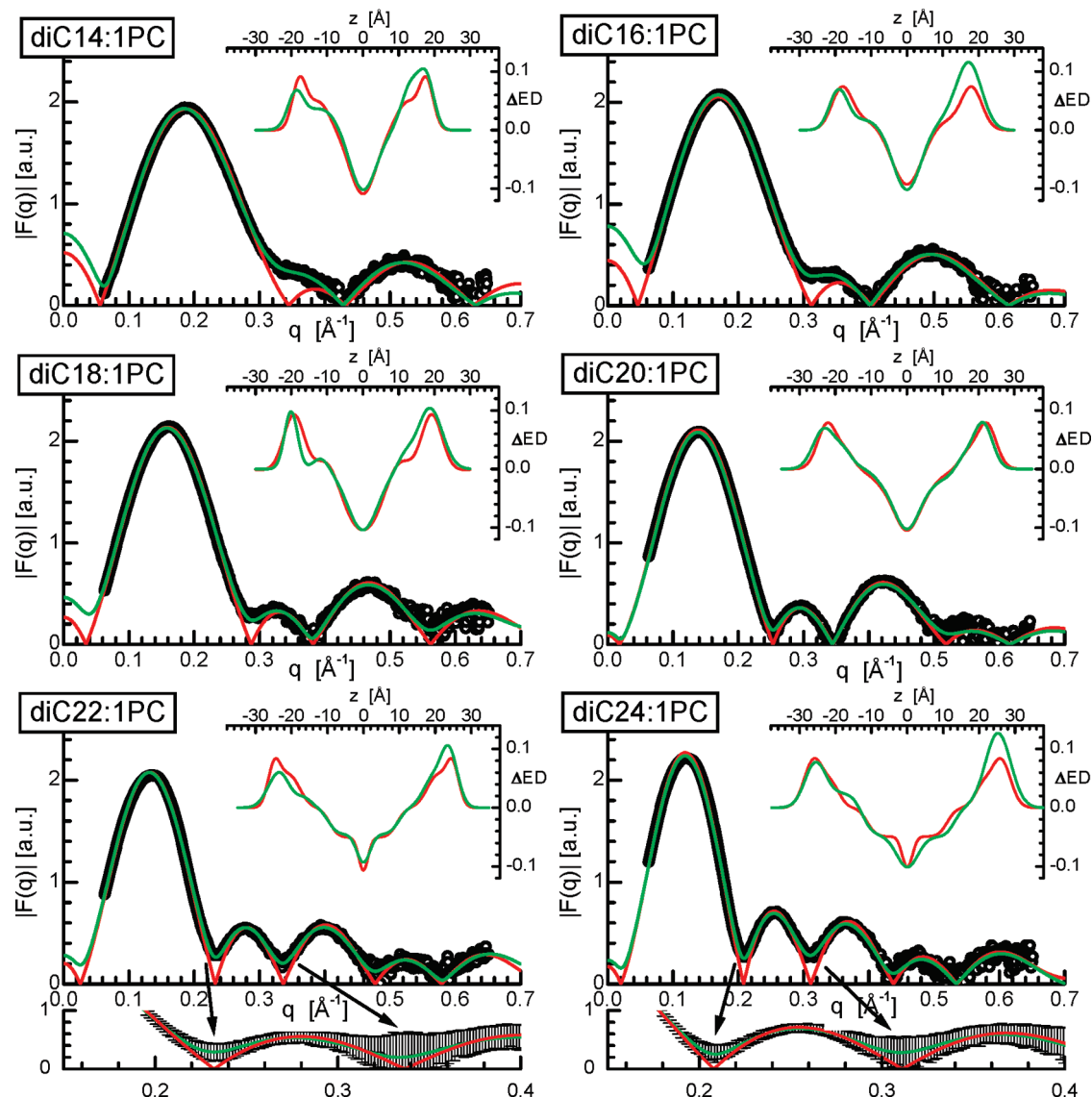


**Figure 2.** The solid lines are best fit results to X-ray scattering form factors  $F(q)$  obtained for di-monounsaturated phosphatidylcholine bilayers with 44 mol % cholesterol at 30 °C. Inset graphs show the water-subtracted 1D electron density profiles. The red curves are best fits to the data using a symmetric bilayer model, while the green curves are best fits to the data using an asymmetric bilayer model. In the case of diC22:1PC and diC24:1PC bilayers, the data are expanded to include the appropriate error bars.

**Binary Mixtures.** Figure 2 shows 1D EDPs for the lipids discussed, but this time with the addition of 44 mol % cholesterol. The differences between the scattering curves in Figure 1 are obvious. The data corresponding to diC14:1PC, diC16:1PC, and diC18:1PC bilayers show very prominent deviations of their second minima from zero intensity (Figure 2). This change in scattered intensity as result of cholesterol could only be fit using the asymmetric bilayer model. In the case of asymmetric bilayers, both the position of the phosphatidylcholine peaks and their associated areas differ considerably between the two bilayer leaflets (see also Table 1). In addition, one of the peaks has split into two, suggesting a significant rearrangement of the phosphatidylcholine headgroups within one of the bilayer's leaflets, most likely the result of cholesterol preferentially partitioning in to one of them.

Although we can speculate that cholesterol partitions preferentially in the inner, more curved bilayer leaflet, because of its affinity for curved regions,<sup>25</sup> we cannot make this conclusion as

scattering data at much smaller  $q$  would be needed in order to extract information regarding the overall ULV structure, and the nature of bilayer asymmetry. Nevertheless, because the changes in an asymmetric bilayer are relatively small (just a few angstroms), it is possible that even if we had smaller  $q$  data, we would not be able to differentiate between the inner or outer bilayer leaflets.

Lipid bilayers whose hydrocarbon chains contain  $\geq 20$  carbons do not form asymmetric bilayers (Figure 2). In the case of diC20:1PC bilayers, the scattering form factors contain minima that are equal to zero, suggesting a symmetric bilayer structure, as also suggested by the 1D EDP (inset to figure). For the lipids with the two longest hydrocarbon chains (i.e., diC22:1PC and diC24:1PC), their scattering data contain minima that deviate from zero; however, these deviations are within experimental error.

## Discussion and Conclusions

It is assumed that single-component, planar lipid bilayers form symmetric structures, but it is not always the case in ULVs.<sup>13,26</sup>

(25) Wang, W.; Yang, L.; Huang, H. W. *Biophys. J.* **2007**, *92*, 2819–2830.

(26) Brzustowicz, M. R.; Brunger, A. T. *J. Appl. Crystallogr.* **2005**, *38*, 126–131.

**Table 1. Structural Parameters of 600 Å ULV Bilayers Made of Monounsaturated PCs without and with Cholesterol (44 mol %)**

bilayers	symmetry	first leaflet		second leaflet		total thickness [Å]
		position [Å]	width [Å]	position [Å]	width [Å]	
diC14:1PC	symmetric	14.7	2.7			29.4
+cholesterol	asymmetric	18.8	2.1	18.0	2.1	36.8
diC16:1PC	symmetric	16.0	2.8			32.0
+cholesterol	asymmetric	19.1	2.5	17.5	3.5	36.6
diC18:1PC	symmetric	17.5	2.9			35.0
+cholesterol	asymmetric	20.1	1.8	18.7	3.5	38.8
diC20:1PC	symmetric	19.9	3.0			39.8
+cholesterol	symmetric	22.4	2.6			44.8
diC22:1PC	symmetric	21.9	3.0			43.8
+cholesterol	symmetric	24.9	1.7			49.8
diC24:1PC	asymmetric	26.6	4.3	21.8	2.6	48.4
+cholesterol	symmetric	26.0	2.7			52.0

For example, it was shown that charged lipids (e.g., phosphatidylserine diC18:1PS) form asymmetric structures in which one bilayer leaflet was found to be thinner than the other. On the other hand, in the case of a neutral lipid with same length hydrocarbon chains (i.e., diC18:1PC), bilayers were shown to be unaffected by bilayer curvature, a result that can be rationalized by simple geometric arguments.<sup>13</sup> Our present results have shown that single-component lipid bilayers made of di-monounsaturated phosphatidylcholines with hydrocarbon chain lengths C14 to C22, form symmetric bilayers. However, our results also indicate that bilayer symmetry breaks down in the case of diC24:1PC, where its two bilayer leaflets exhibit different lipid densities and thicknesses, most likely as a result of bilayer curvature.

The addition of cholesterol to the above-mentioned bilayers also produced some very interesting results. Importantly, it seems that cholesterol, by distributing itself unequally between the bilayer's two leaflets, induces bilayer asymmetry in symmetric bilayers whose hydrocarbon chains contain  $\leq 18$  carbons. These results are in good agreement with MD simulations,<sup>19</sup> which stated that up to 2/3 of cholesterol molecules are located in one of the bilayer's leaflets. This translates in to a lipid/cholesterol ratio of 2 in one leaflet, while in the other leaflet this ratio is almost 4. Figure 3 shows a schematic of such a bilayer, which has been overlaid with the 1D EDP calculated from experimental data. Note that the cholesterol concentration in any one leaflet is still below the equilibrium maximum solubility of cholesterol, which is about 1.5 phosphatidylcholines per cholesterol.<sup>27</sup>

It is interesting to note that the magnitude of bilayer asymmetry coincides with the difference in length between the lipid's hydrocarbon chains and cholesterol. Asymmetry is most pronounced in the thinnest bilayer (i.e., diC14:1PC) whose hydrocarbon thickness is significantly shorter than a cholesterol molecule.<sup>19</sup> With decreasing hydrophobic mismatch, however, we observe a decrease in cholesterol's asymmetric distribution, eventually distributing itself equally between the two leaflets of diC20:1PC bilayers. Table 1 suggests that symmetric bilayers are formed when the bilayer's hydrocarbon thickness is close to the length of cholesterol. It is possible that, in addition to bilayer disorder discussed above, hydrophobic mismatch is another important factor in the asymmetric distribution of cholesterol.

The effect on bilayer asymmetry induced by cholesterol is best appreciated by looking at the 1D EDPs. First, the bilayer leaflets differ in thickness (see also Table 1). It is known that cholesterol increases bilayer thickness by decreasing chain disorder;<sup>28,29</sup> we therefore infer that the thicker leaflet contains more cholesterol.

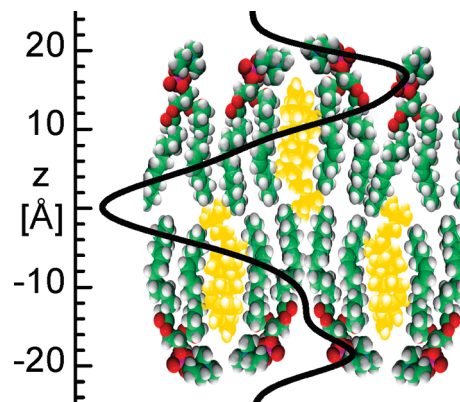


**Figure 3.** diC14:1PC bilayers with cholesterol (yellow). The schematic shows an unequal (2:1) distribution of cholesterol between the two bilayer leaflets. The solid line overlaying the bilayer corresponds to the 1D electron density profile (EDP) calculated from experimental data.

Second, the peak corresponding to the lipid headgroup's phosphate happens to be sharper in the thicker leaflet, suggesting a major rearrangement of lipid headgroups upon the addition of cholesterol. This rearrangement, we believe, is best described by the "umbrella model",<sup>30</sup> whereby lipid headgroups in the presence of cholesterol reorient to shield the cholesterol thus avoiding an energetically unfavorable contact of cholesterol with water, as was recently observed in MD simulations of diC14:1PC and diC22:1PC lipid bilayers with cholesterol.<sup>19</sup> We also note that the lipid headgroup peak widths should get narrower with additional ordering, which is what is observed for all bilayers with cholesterol.

In summary, from SAXS experiments we have been able to detect the formation of asymmetric lipid bilayers in 600 Å diameter ULVs. We find that bilayers made of di-monounsaturated phosphatidylcholine lipids (diC $n$ :1PC, where  $n = 14-22$ ) form commonly observed symmetric bilayers, while this symmetry breaks down in the case of diC24:1PC bilayers. Interestingly, the addition of 44 mol % cholesterol induces bilayer asymmetry in shorter hydrocarbon chain bilayers (C14 to C18), effectively through the unequal distribution of cholesterol between the bilayer's two leaflets. As a similar asymmetry was not previously found in planar bilayers, we attribute this effect to the curvature present in ULV bilayers. This result, we believe, is of relevance to biological membranes which consist of a wide variety of lipids with different intrinsic properties. Although it is still not clear whether local curvature affects lipid composition, or

(27) Huang, J.; Buboltz, J. T.; Feigenson, G. W. *Biochim. Biophys. Acta* **1999**, *1417*, 89–100.

(28) Levine, Y. K.; Wilkins, M. H. *Nat. New Biol.* **1971**, *230*, 69–72.

(29) McIntosh, T. J. *Biochim. Biophys. Acta* **1978**, *513*, 43–58.

(30) Huang, J.; Feigenson, G. W. *Biophys. J.* **1999**, *76*, 2142–2157.

vice versa, the resultant structural changes that may take place as a result of differing lipid properties may be important in the regulation of protein function.

**Acknowledgment.** The authors acknowledge Dr. Arthur Woll for assistance with the G-line SAXS setup at the Cornell High

Energy Synchrotron Source (CHESS), which is funded by a National Science Foundation Grant DMR-0225180.

**Supporting Information Available:** Data analysis. This material is available free of charge via the Internet at <http://pubs.acs.org>.